



# La-Metal-Organic Framework incorporating Fe<sub>3</sub>O<sub>4</sub> nanoparticles, post-synthetically modified with Schiff base and Pd. A highly active, magnetically recoverable, recyclable catalyst for C–C cross-couplings at low Pd loadings

Gang Xiong<sup>a</sup>, Xiao-Ling Chen<sup>a</sup>, Li-Xin You<sup>a</sup>, Bao-Yi Ren<sup>a</sup>, Fu Ding<sup>a</sup>, Ileana Dragutan<sup>b</sup>, Valerian Dragutan<sup>b,\*</sup>, Ya-Guang Sun<sup>a,\*</sup>

<sup>a</sup>The Key Laboratory of Inorganic Molecule-Based Chemistry of Liaoning Province, Shenyang University of Chemical Technology, Shenyang 110142, China

<sup>b</sup>Institute of Organic Chemistry, Romanian Academy, Bucharest 060023, Romania

## ARTICLE INFO

### Article history:

Received 21 November 2017

Revised 22 February 2018

Accepted 26 February 2018

### Keywords:

Metal-organic framework (MOF)

Fe<sub>3</sub>O<sub>4</sub>

Post-synthetic modification

Heterogeneous palladium catalyst

Magnetically recoverable

Suzuki-Miyaura cross-coupling

## ABSTRACT

Unprecedented post-synthetic modification (PSM) applied on a new La-MOF containing Fe<sub>3</sub>O<sub>4</sub> nanoparticles (NPs), via Schiff base build-up (with pyridine-2-carboxaldehyde) and PdCl<sub>2</sub> coordination, proved to be an advantageous strategy to produce a superior heterogeneous catalyst for Suzuki-Miyaura C–C bond formation. The Fe<sub>3</sub>O<sub>4</sub>@La-MOF-Schiff base-Pd ensemble (characterized by PXRD, EDS, TEM, HAADF-STEM, VSM, TGA) showed very active, quite stable, magnetically recoverable and reusable in coupling of bromo- or iodoaryls with arylboronic acids, affording practically quantitative yields of biaryls (>99%) and high TONs and TOFs. The catalyst has been recycled up to 12 times without significant loss of the catalytic activity. A synergistic cooperativity between Pd and the oxophilic La nodes, through the organic linker, is responsible for enhancing the catalytic activity and stability.

© 2018 Elsevier Inc. All rights reserved.

## 1. Introduction

As a new type of highly tailorable microporous materials, metal-organic frameworks (MOFs) are at the core of a variety of specific applications such as catalysis [1], gas storage [2], drug delivery [3a], sensors [3b] or diversified multifunctional materials [4]. In particular, MOFs have played a key role in heterogeneous catalysis as catalyst templates due to their high surface area, adjustable pore size, robustness, controllable distribution of the catalytically active sites, and increased activity and chemoselectivity [1,5]. Furthermore, post-synthetic modification (PSM) of MOFs has emerged as an important tool for introducing a wide range of functional groups into the complex MOF superstructures extending thus their use in catalysis according to current needs [6–8]. Presently, there are two PSM strategies for MOF functionalization. In the first, the newly introduced functions are connected to backbones of the MOFs by covalent, coordination or covalent-coordination modification [9,10]. For instance, amine groups on

MOFs, as target motifs, are frequently reacted with anhydrides [11,12] and aldehydes [13–15] via PSM to create multidentate coordination sites. The latter can further coordinatively bind metal ions, catalytically active, such as Pd (II), in view of efficient application in C–C cross couplings. The second method is to load nanoparticles, such as Au, Pt, Ni and Cu, in the void spaces of MOFs by the method of impregnation in metal salt solutions and reduction, then use the resulting modified MOFs as catalysts in well-defined reactions [16a]. However, a method implying the two above mentioned strategies for tailoring La-MOFs, which might further widen the perspectives of valorising these unique materials, has not been previously [16b] reported.

Palladium-catalyzed cross-couplings, conducted in homogeneous and heterogeneous phase, have been extensively applied in synthetic chemistry [17–21]. Among these, Suzuki-Miyaura cross-coupling of aryl halides with arylboronic acids represents an efficient way for forming carbon-carbon bonds, particularly for synthesis of biaryls as building blocks of pharmaceutical products [17]. In spite of this progress, isolation of homogenous catalysts from reaction mixtures is sometimes quite difficult and metal leaching is problematic leading to highly toxic palladium (II) residues [21a]. Although development of heterogeneous

\* Corresponding authors.

E-mail addresses: [vdragutan@yahoo.com](mailto:vdragutan@yahoo.com) (V. Dragutan), [sunyaguang@syuct.edu.cn](mailto:sunyaguang@syuct.edu.cn) (Y.-G. Sun).

catalytic systems made it possible to isolate and recycle the recovered catalysts, some Pd leaching and cumbersome processes such as filtration and clogging still remain current issues that affect the reuse of conventional heterogeneous catalysts, especially when solid inorganic bases are employed. To meet these challenges, catalysts supported on magnetic nanoparticles (MNPs) offered a convenient use circumventing separation by centrifugation or tedious filtration, the catalyst being instead recovered simply by applying an external magnet [22]. Thus, Zhang and coworkers [23a] synthesized a palladium-2,2-bipyridine complex supported on  $\text{Fe}_3\text{O}_4$  nanoparticles and valorised it in Suzuki-Miyaura couplings. This catalyst could be easily separated magnetically. More recently, Astruc and coworkers [23b] took advantage of magnetically recoverable “click” PEGylated  $\gamma\text{-Fe}_2\text{O}_3\text{-Pd}$  nanoparticle catalysts in the Suzuki-Miyaura, Sonogashira, and Heck reactions, demonstrating intervention of strong positive dendritic effects on catalyst loading, catalytic activity, and recyclability. Also, superparamagnetic polymer composite microspheres ( $\text{Fe}_3\text{O}_4/\text{polymer}$ ), used to support palladium nanoparticles, provided high reactivity in Suzuki coupling reactions, while the catalyst could be easily recovered and reused for five times [23c]. Further notable applications of Pd on magnetic supports as catalysts in C–C bond formation have also been reported [23d,23e].

Prompted by these developments and continuing our research program on Pd-catalyzed cross-coupling reactions [18b,19b,19c], we have designed a highly efficient  $\text{Fe}_3\text{O}_4$  nanoparticle-supporting catalyst, synthesized via a PSM strategy operated on a La-MOF [La(abdc)(HabdC) $\cdot$ 9H $_2$ O] $_n$  (abdc = 2-amino-benzene-1,4-dicarboxylate), herein reported for the first time (Scheme 1). The significant robustness and fine porosity of this La-MOF, provided by the oxophilic La nodes and dicarboxylic organic linker, coupled with adequate stability to solvents and chemical reagents, were good reasons for choosing it as substrate for PSM [24–26]. Besides, our synthesis protocol is very simple so that this new catalyst can be made available on a large scale.

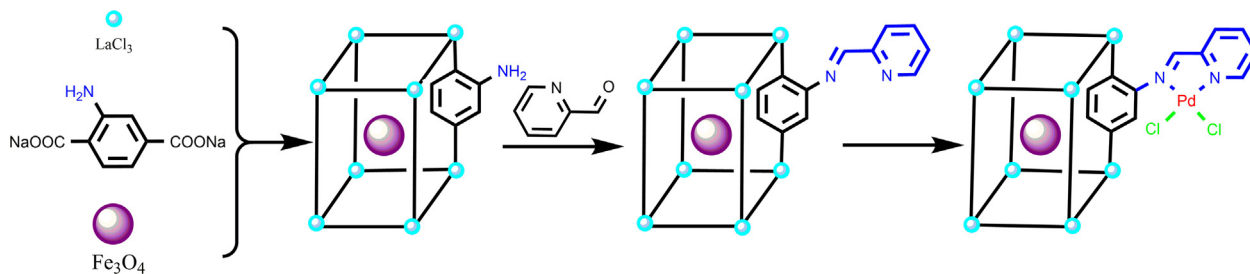
## 2. Experimental

### 2.1. Catalyst preparation

All starting materials and solvents were obtained and used without further purification from commercial suppliers.

#### 2.1.1. Synthesis of disodium 2-amino-benzene-1,4-dicarboxylate

Two equivalents of sodium hydroxide were added to a suspension of 2-amino-benzene-1,4-dicarboxylic acid ( $\text{H}_2\text{abdc}$ ) in distilled water and the mixture stirred until all components were fully dissolved. After adjusting the pH of the solution to 6 and heating it carefully in air to dryness, a pale yellow powder of disodium 2-aminoterephthalate was collected.



Scheme 1. Synthesis route of  $\text{Fe}_3\text{O}_4@$ La-MOF-Schiff base-Pd.

#### 2.1.2. Synthesis of magnetic $\text{Fe}_3\text{O}_4$ nanoparticles

$\text{FeCl}_3\cdot 6\text{H}_2\text{O}$  (2.7 g) and  $\text{FeSO}_4\cdot 7\text{H}_2\text{O}$  (2.7 g) were added to distilled water (60 mL) and stirred until all the components were dissolved. A brown precipitate was generated by adding the right amount of  $\text{NH}_3\cdot \text{H}_2\text{O}$  (28%), under mechanical stirring. After adjusting the pH to 10, the solution was heated at 80 °C for 0.5 h. The  $\text{Fe}_3\text{O}_4$  was collected and washed 3 times with distilled water and 3 times with ethanol. After drying, the obtained black  $\text{Fe}_3\text{O}_4$  powder (1.5987 g) was dispersed into ethanol at a concentration of 7 mg/mL.

#### 2.1.3. Synthesis of microcrystalline powder La-MOF

A microcrystalline powder of La-MOF was obtained by mixing in water stoichiometric amounts of lanthanide chloride and disodium 2-amino-benzene-1,4-dicarboxylate. Precipitation immediately occurred and the pale-yellow precipitate was filtered and dried in air.

#### 2.1.4. Synthesis of single crystal La-MOF

$\text{NaOH}$  (0.1 M) was added dropwise to 10 mL water solution of  $\text{H}_2\text{abdc}$  (0.018 g, 0.10 mmol) adjusting the pH value to 5–6, and the resulting solution was introduced into a test tube. A new solution of  $\text{La}(\text{NO}_3)_3\cdot 6\text{H}_2\text{O}$  (0.044 g, 0.10 mmol) in 2-propanol (8 mL) was allowed to slowly diffuse into the above solution of  $\text{H}_2\text{abdc}$  through a buffering layer of 2-propanol and water (1:1). Colorless cubic crystals suitable for X-ray crystal analyses were obtained after four days (yield 20%), which are stable in air and insoluble in water and common organic solvents

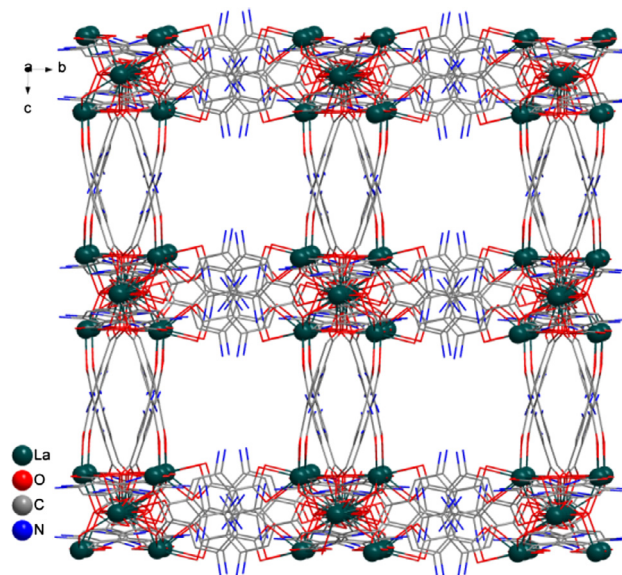


Fig. 1. The 3D structure of La-MOF highlighting the 4-nodal topology of the La-MOF subunit.

### 2.1.5. Synthesis of the $\text{Fe}_3\text{O}_4@La\text{-MOF}$

A suspension of nanosized  $\text{Fe}_3\text{O}_4$  (7 mg/mL, 50 mL; see Section 1.2) was added to a solution of  $\text{LaCl}_3 \cdot 6\text{H}_2\text{O}$  (2.1201 g) in distilled water (20 mL), under mechanical stirring. After a few minutes, a solution of disodium 2-amino-benzene-1,4-dicarboxylate (2.7014 g) in distilled water (20 mL) was added under mechanical stirring; immediately a brown precipitate was generated. The brown precipitate was collected and washed 3 times each with distilled water and ethanol. Then the brown precipitate was isolated by using a magnet and dried to give  $\text{Fe}_3\text{O}_4@La\text{-MOF}$  (3.1039 g).

### 2.1.6. Synthesis of $\text{Fe}_3\text{O}_4@La\text{-MOF-Schiff base}$

A mixture of  $\text{Fe}_3\text{O}_4@La\text{-MOF}$  (2.7133 g), pyridine-2-carboxaldehyde (8 mmol) and ethanol (100 mL) was mechanically stirred for 2 days. The formed precipitate was collected and

washed with distilled water and ethanol for 3 times each. Then the brown precipitate was isolated by using an external magnet and dried in air to give the brown  $\text{Fe}_3\text{O}_4@La\text{-MOF-Schiff base}$  (2.5825 g).

### 2.1.7. Synthesis of $\text{Fe}_3\text{O}_4@La\text{-MOF-Schiff base-Pd}$

A mixture of  $\text{Fe}_3\text{O}_4@La\text{-MOF-Schiff base}$  (1.9636 g),  $\text{PdCl}_2$  (0.2215 g) and ethanol (100 mL) was mechanically stirred for 2 days, at room temperature. The precipitate was collected and washed with distilled water and ethanol for 3 times, respectively. Then the brown precipitate was isolated by using a magnet and dried to give the brown  $\text{Fe}_3\text{O}_4@La\text{-MOF-Schiff base-Pd}$  (1.8921 g).

## 2.2. General reaction conditions for the Suzuki-Miyaura cross-coupling reactions

The typical experimental procedure for the Suzuki-Miyaura coupling reactions using the  $\text{Fe}_3\text{O}_4@La\text{-MOF-Schiff base-Pd}$  as catalyst is as follows. A mixture of aryl halide (1 mmol), boronic acid (1.2 mmol), base (2.0 mmol, the indicated species), solvent (6 mL, as indicated) and catalyst (the given amount) were placed in a Schlenk tube and stirred in air, at the appropriate temperature for the certain time (as indicated in Tables 1–3, S3 and S4). After completion of the reaction, a magnet was used to separate the catalyst and then the mixture was extracted three times with ethyl acetate. The product yield was determined by gas chromatography (GC) analysis using hexadecane as the internal standard.

## 2.3. Characterization

Powder X-ray diffraction (PXRD) patterns of the samples were collected on an X-ray diffractometer (BRUKER D8 ADVANCE) with Cu K radiation. Thermal Gravimetric experiments were carried out on a SDT Q600 instrument with a heating rate of 10 °C/min. The

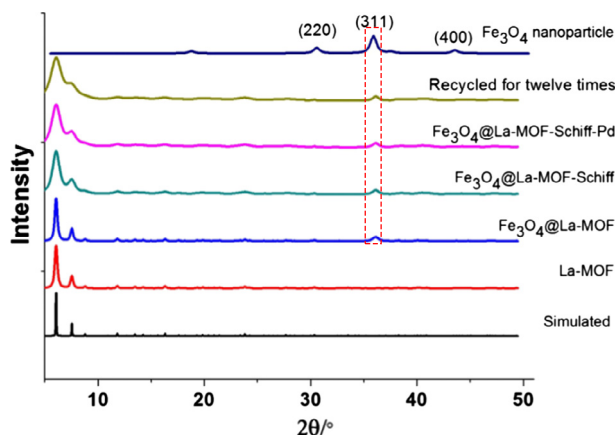


Fig. 2. PXRD patterns for different samples indicating the presence of  $\text{Fe}_3\text{O}_4$  NP in the catalyst.

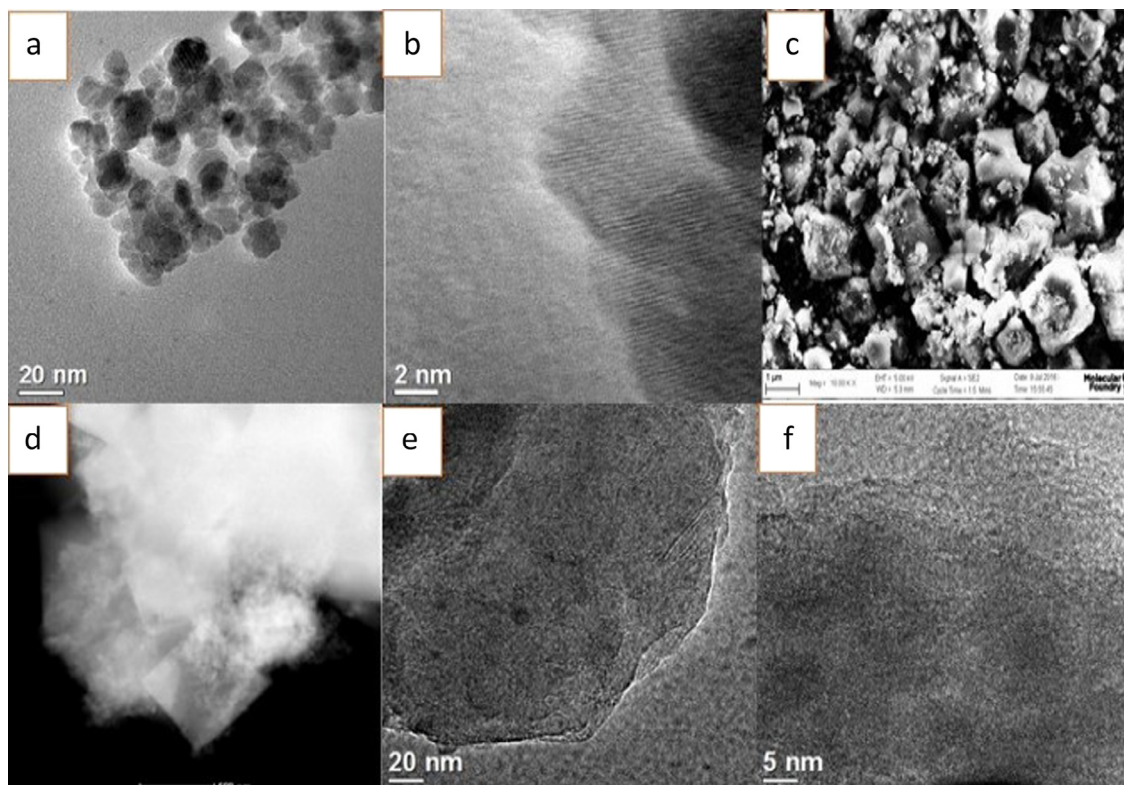


Fig. 3. (a and b) TEM image of the  $\text{Fe}_3\text{O}_4$  nanoparticles; (c) SEM of  $\text{Fe}_3\text{O}_4@La\text{-MOF-Schiff base-Pd}$ ; (d) STEM of  $\text{Fe}_3\text{O}_4@La\text{-MOF-Schiff base-Pd}$ ; (e-f) TEM image of  $\text{Fe}_3\text{O}_4@La\text{-MOF-Schiff base-Pd}$ .

magnetic measurements were carried out by VSM at room temperature.  $N_2$  gas sorption experiments were carried out on a V-Sorb 2800 TP volumetric gas sorption instrument. GC analyses were performed on an Agilent Technologies 7890A gas chromatograph. X-ray photoelectron spectroscopy was determined on Thermo VG ESCALAB250. ICP-AES was determined on Thermo IRIS Advantage. SEM images were taken with a Zeiss Gemini Ultra-55 analytical scanning electron microscope at an accelerating voltage of 5 keV. Energy-dispersive X-ray spectroscopy (EDS) was taken on a Zeiss Gemini Ultra-55 analytical scanning electron microscope with an EDAX EDS detector with Genesis software. TEM images were taken on a JEOL 2100F operated at 120 keV equipped with Gatan Tridiem imaging spectrometer. High-angle annular dark-field (HAADF) scanning TEM (STEM) investigations using high angle annular dark-field STEM (HAADF-STEM) were acquired with a 1-nm probe at 200 kV with a monochromated FEI Tecnai F20 scanning-trans

mission-electron-microscope (STEM).  $^1H$  NMR spectra were recorded on a Bruker BioSpin GmbH AVANCE III 500 MHz spectrometer operating at 500 MHz.

A suitable crystal was selected and mounted on a SuperNova, Single source at offset, Eos diffractometer with a graphite-monochromatic  $MoK\alpha$  radiation ( $\lambda = 0.71073 \text{ \AA}$ ) using the  $\omega$ -scan technique. The crystal was kept at 120 K during data collection. Using Olex2<sup>1</sup>, the structure was solved with the Superflip<sup>2</sup> structure solution program using Charge Flipping and refined with the XL<sup>3</sup> refinement package using Least Squares minimisation. The occupancy sum of N1, N2, N3 atoms is 1. Hydrogen atoms of free water molecules have not been localized. Crystal and final structure refinements of single crystal La-MOF have been listed in Table S1. CCDC: 1522121. The data can be obtained free of charge from the Cambridge Crystallographic Data Centre via [www.ccdc.cam.ac.uk/data\\_request/cif](http://www.ccdc.cam.ac.uk/data_request/cif).

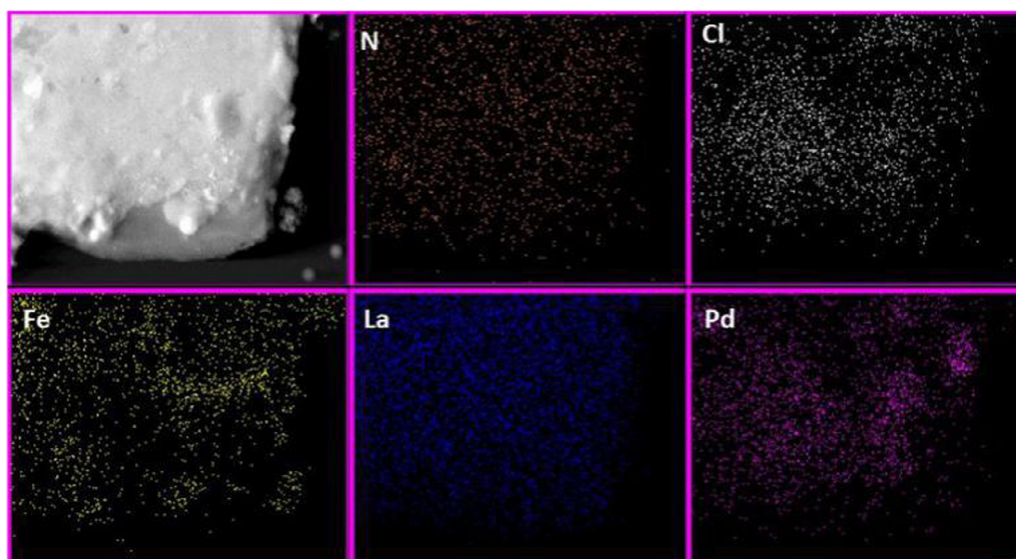


Fig. 4. HAADF-STEM image and elemental mappings of  $Fe_3O_4@La$ -MOF-Schiff base-Pd show the presence of N, Cl, Fe, La and Pd atoms in the catalyst.

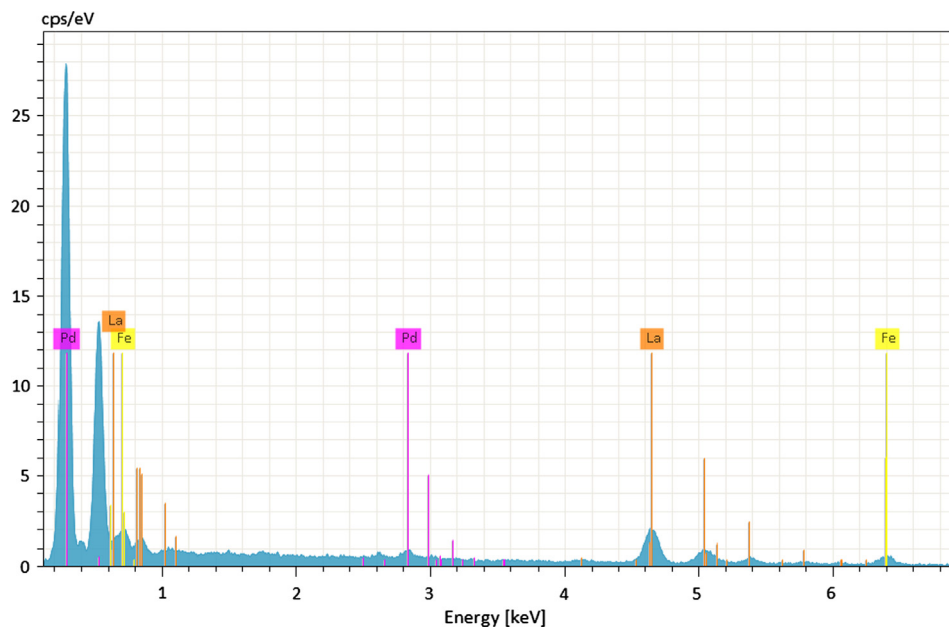


Fig. 5. EDS spectrum of  $Fe_3O_4@La$ -MOF-Schiff base-Pd.

### 3. Results and discussion

The X-ray structure analysis on a single crystal reveals that La-MOF crystallized in the cubic system, space group  $Ia-3$  (Table S1). It presents a *pcu* topology 3D framework composed of *abdc* linkers and linear tri-nuclear La units, which is isostructural to the known neodymium compound  $[\text{Nd}(\text{abdc})(\text{Habdc})\cdot 9\text{H}_2\text{O}]_n$  [27]. The layered structure of the powder La-MOF (Figs. 1 and S1) was confirmed by PXRD analysis, as compared with single-crystal structure of La-MOF.

$\text{Fe}_3\text{O}_4$ @La-MOF has been readily synthesized by mixing aqueous solutions of  $\text{LaCl}_3$ , disodium 2-aminobenzene-1,4-dicarboxylate and  $\text{Fe}_3\text{O}_4$  nanoparticles under gentle mechanical stirring.  $\text{Fe}_3\text{O}_4$ @La-MOF was post-synthetically modified first by reaction with pyridine-2-carboxaldehyde to give the imine derivative  $\text{Fe}_3\text{O}_4$ @La-MOF-Schiff base, and then by coordination with  $\text{PdCl}_2$  to afford the palladium-functionalized framework  $\text{Fe}_3\text{O}_4$ @La-MOF-Schiff base-Pd.

Powder X-ray diffraction (PXRD) (Fig. 2) illustrates that  $\text{Fe}_3\text{O}_4$  nanoparticles have been successfully embedded in the La-MOF while the crystalline state of the backbones was kept during post-synthetic modification. Noteworthy, the characteristic signal of  $\text{Fe}_3\text{O}_4$  nanoparticles was present in the PXRD even after recycling the catalyst for twelve times.

TGA curves (Fig. S2) demonstrate a considerable thermal stability of the post-synthetically modified MOF. The  $\text{N}_2$  adsorption-desorption isotherms (Fig. S3) showed a decrease of the BET surface areas paralleling the different stages of the catalyst preparation. According to data in Table S2, there is about a  $50\text{ m}^2/\text{g}$  difference in BET surface areas between La-MOF and  $\text{Fe}_3\text{O}_4$ @La-MOF indicating that  $\text{Fe}_3\text{O}_4$  has been primarily encapsulated into La-MOF, as also confirmed from the TEM spectrum (Fig. 3a and b). The relatively low content and small size of  $\text{Fe}_3\text{O}_4$  nanoparticles are responsible for encapsulation and the first

decrease in the BET surface. A further slighter decrease in the BET surface ( $32\text{ m}^2/\text{g}$ ) occurs after PSM with the Schiff base, assigned to the effect of functionalization. However, the remaining, still high, surface area will be conducive to an efficient spread of the tethered Pd catalytic sites.

The cube morphology of  $\text{Fe}_3\text{O}_4$ @La-MOF-Schiff base-Pd (Fig. 3c and d), similar to that of La-MOF (Fig. S4), evidences the maintenance of the crystalline state. As in Fig. 3a, the black dots in Fig. 3e and f represent embedded  $\text{Fe}_3\text{O}_4$  nanoparticles. From TEM analysis (Fig. 3a and b) and SEM image (Fig. S4(a)) of the  $\text{Fe}_3\text{O}_4$  nanoparticles, it was inferred that their size is about 10 nm. The typical TEM image of  $\text{Fe}_3\text{O}_4$ @La-MOF-Schiff base-Pd, as well as the corresponding elemental mappings for the synthesized catalyst (shown in Fig. 4), testify for an even distribution of the  $\text{Fe}_3\text{O}_4$  nanoparticles and of Pd ions in the composite, crucial for a superior performance of the heterogeneous promoter.

The obvious conclusion is that the  $\text{Fe}_3\text{O}_4$  nanoparticles are correspondingly embedded in the interior of the La-MOF. The content of  $\text{Fe}_3\text{O}_4$  in  $\text{Fe}_3\text{O}_4$ @La-MOF has been determined to be ca. 11 wt%. In the  $\text{Fe}_3\text{O}_4$ @La-MOF-Schiff base-Pd, the amount of  $\text{Fe}_3\text{O}_4$  corresponds to a value of 9.35 wt% (considering the total weight of the catalyst, after PSM with Schiff base and Pd). The EDS spectrum showed, as expected, the concomitant presence of Fe, La and Pd species (Figs. 5 and S5).

The magnetization saturation value of  $37.9\text{ emu}\cdot\text{g}^{-1}$ , taken from the magnetic hysteresis loop curve of  $\text{Fe}_3\text{O}_4$ @La-MOF-Schiff base-Pd (Fig. S6), evidences that the catalyst can be easily separated from the reaction mixture, just by an external magnet. The binding energy (400 eV) of N atoms in the  $\text{Fe}_3\text{O}_4$ @La-MOF-Schiff base (inferred from XPS measurements) is slightly higher as compared to that in  $\text{Fe}_3\text{O}_4$ @La-MOF-Schiff base-Pd (Fig. S7). The rationale would be that electrons are transferred from N atoms to Pd atoms, thus providing further support for a suitable coordination of palladium atoms to the N atoms resulting in a good stability of the Pd

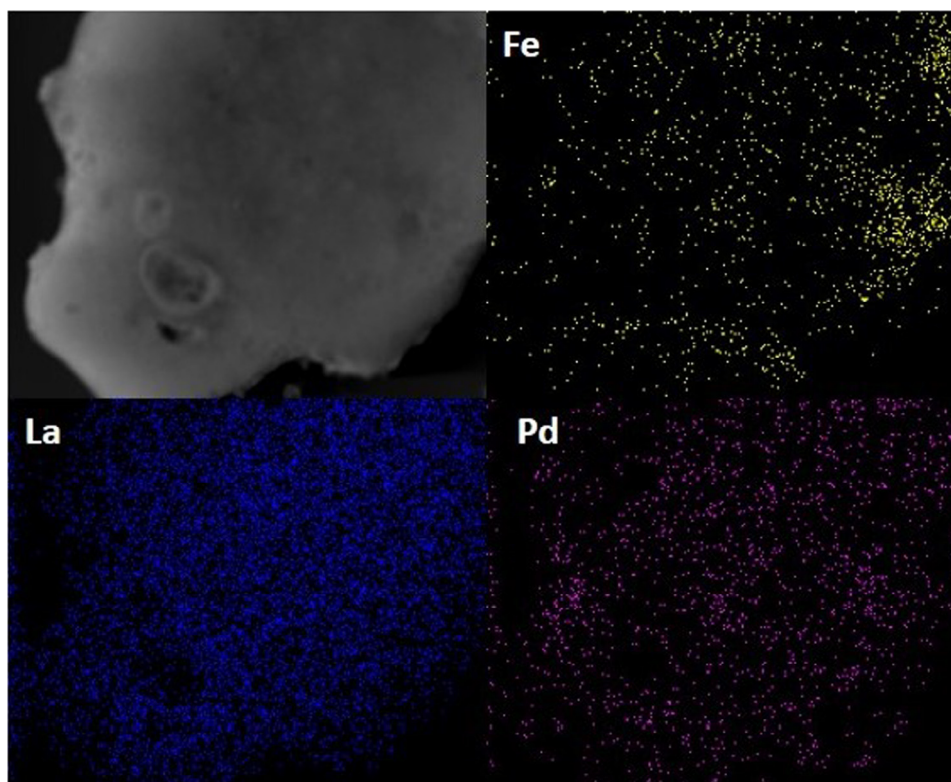


Fig. 6. HAADF-STEM images of the recovered  $\text{Fe}_3\text{O}_4$ @La-MOF-Schiff base-Pd.

complex. From an ICP-AES measurement on  $\text{Fe}_3\text{O}_4@La\text{-MOF-Schiff base-Pd}$  we could deduce a palladium content of 0.873 wt% ( $8.23 \times 10^{-3}$  mol% Pd). The actual distribution of Fe, La and Pd within the catalyst, before and after use, could be properly evaluated from the HAADF-STEM (Figs. 6 and S8) and TEM images (Figs. 7 and S9). From Fig. 7a and c, as well as from Fig. S8, it appears that the size of recovered  $\text{Fe}_3\text{O}_4@La\text{-MOF-Schiff base-Pd}$  has not been changed. Practically, the morphology of the catalyst was destroyed by the prolonged mechanical stirring, but PXRD indicated that the catalyst was not decomposed. As inferred from the XPS (Fig. S10), the valence of Pd is +2.

Overall, these determinations indicate that the catalyst has been successfully prepared and used in cross-coupling reactions according to our pre-established protocol.

The catalytic activity of the  $\text{Fe}_3\text{O}_4@La\text{-MOF-Schiff base-Pd}$  was investigated in the Suzuki-Miyaura cross-couplings of selected aryl halides with arylboronic acids (Table 1). Rewardingly, yields of over 99% in different biaryl products have been attained for both aryl iodides and bromides, under mild conditions. As expected, aryl chlorides gave lower yields, readily accounted for by the reduced reactivity of aryl chlorides in the oxidative addition rate-determining step of the catalytic cycle [28], as compared to their bromide and iodide counterparts.

Products from each stage of the catalyst preparation, *i.e.*  $\text{Fe}_3\text{O}_4$ , La-MOF,  $\text{Fe}_3\text{O}_4@La\text{-MOF}$ ,  $\text{Fe}_3\text{O}_4@La\text{-MOF-Schiff base}$  and  $\text{Fe}_3\text{O}_4@La\text{-MOF-Schiff base-Pd}$ , were in turn used as possible initiators in a standard reaction, between bromobenzene and phenylboronic acid (Table S3). Predictably, results showed that only  $\text{Fe}_3\text{O}_4@La\text{-MOF-Schiff base-Pd}$  acted, due to the presence of palladium active species, as an effective catalyst, at reasonable catalyst loadings (Table 2), the influence played by the catalyst amount, reaction temperature and time have also been minutely examined (Tables 2 and 3). We found that a high yield (95%) could be obtained employing a very small amount of the catalyst (3 mg). By raising the catalyst amount to 8 mg, the yield exceeded 99%, showcasing this catalyst as an excellent promoter of Suzuki-Miyaura C–C bond formation. The particular catalytic ability of  $\text{Fe}_3\text{O}_4@La\text{-MOF-Schiff base-Pd}$  was also far superior to that of  $\text{PdCl}_2$ . Using  $\text{PdCl}_2$  as the catalyst and working under same reaction conditions, a lower yield was obtained (56%), as compared with  $\text{Fe}_3\text{O}_4@La\text{-MOF-Schiff base-Pd}$  (yield >99%) (Table S3). Obviously, in comparison with  $\text{PdCl}_2$ , the  $\text{Fe}_3\text{O}_4@La\text{-MOF-Schiff base-Pd}$  catalyst displays a higher catalytic activity at a lower Pd loading, exhibiting at the same time a substantial robustness, easy magnetic recoverability, 12 times recyclability, and a minimum noble metal leaching.

Optimization of main reaction parameters was further carried out using different bases and solvents (Table S4). Data evidenced that the best combination allowing high yields (>99%) to be attained was  $\text{K}_2\text{CO}_3$  as the base and ethanol as the solvent (Table S4, entry 2). On raising the reaction temperature the yield sharply increased. At 80 °C and a reaction time of 0.5 h, the yield was as high as 99% (Table 3). In conclusion, ethanol as the solvent, potassium carbonate as the base, 8 mg of catalyst, reaction time 0.5 h, and a temperature of 80 °C provide best results.

With a reduced amount of catalyst (1 mg;  $8.23 \times 10^{-3}$  mmol% Pd) and an excess of bromobenzene (2 mmol; Table 1, entry 12),

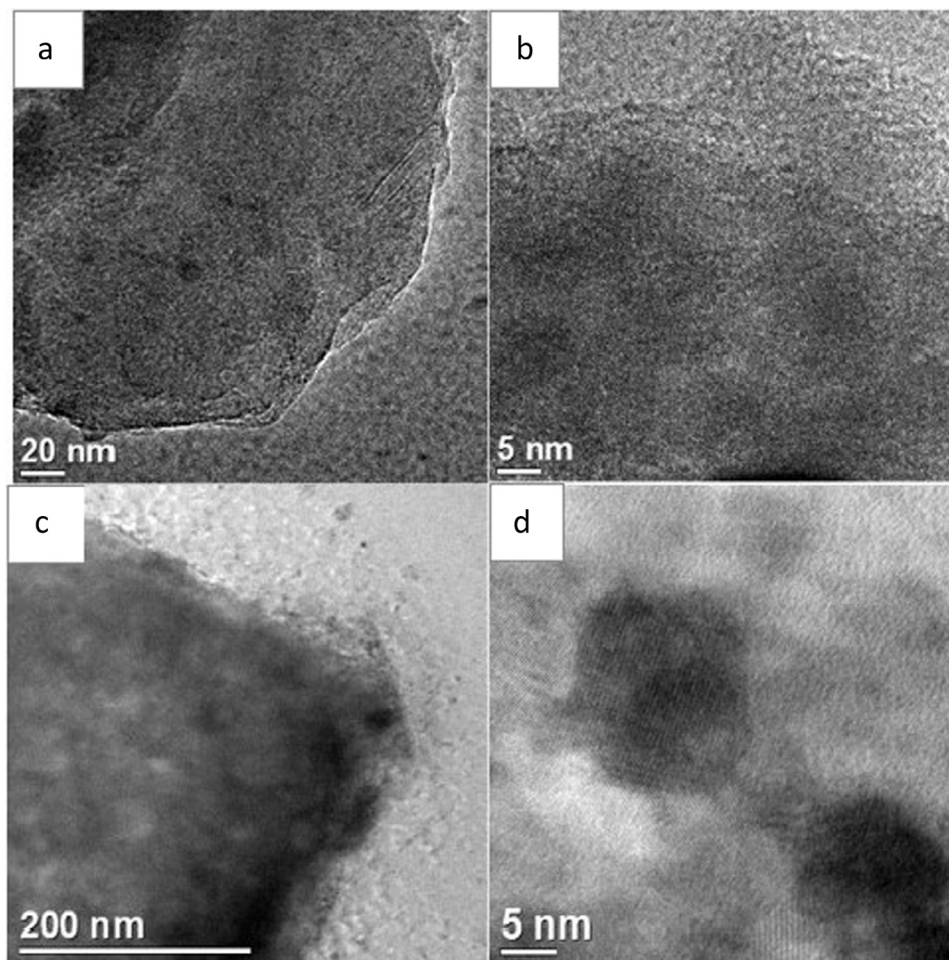
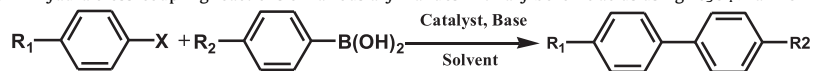
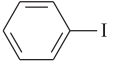
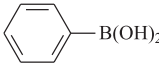
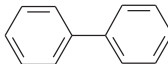
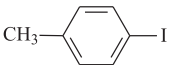
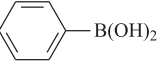
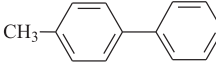
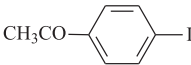
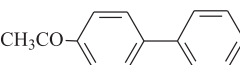
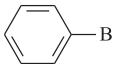
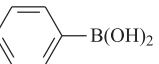
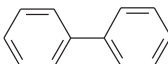
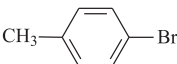
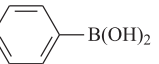
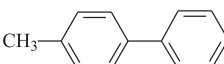
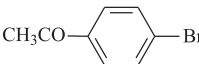
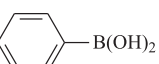
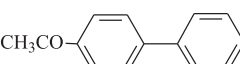
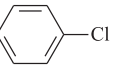
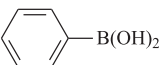
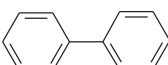
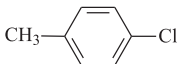
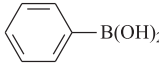
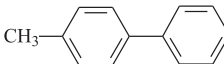
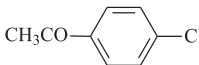
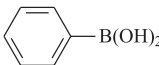
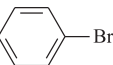
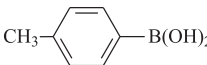
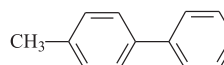
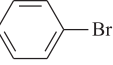
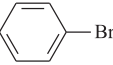
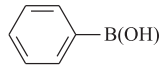
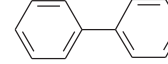


Fig. 7. (a and b) TEM image of  $\text{Fe}_3\text{O}_4@La\text{-MOF-Schiff base-Pd}$  before use; (c and d) TEM image of the recovered  $\text{Fe}_3\text{O}_4@La\text{-MOF-Schiff base-Pd}$ .

**Table 1**Suzuki-Miyaura cross-coupling reactions of various aryl halides with arylboronic acids using Fe<sub>3</sub>O<sub>4</sub>@La-MOF-Schiff base-Pd as catalyst.<sup>a</sup>

Entry	Aryl halide	Arylboronic acid	Product	Yield, %
1				>99
2				99
3				>99
4				>99
5				95
6				>99
7 <sup>b</sup>				5
8 <sup>b</sup>				14
9 <sup>b</sup>				19
10				>99
11				52
12 <sup>c</sup>				88

<sup>a</sup> Reaction conditions: aryl halide (1.0 mmol), arylboronic acid (1.2 mmol), K<sub>2</sub>CO<sub>3</sub> (2.0 mmol), ethanol (6 mL), catalyst (8 mg, 0.066 mmol% Pd), temperature (80 °C), time (0.5 h). <sup>b</sup>Reaction conditions: catalyst (10 mg), temperature (80 °C), time (10 h). <sup>c</sup>Reaction conditions: bromobenzene (2.0 mmol), phenylboronic (2.4 mmol), K<sub>2</sub>CO<sub>3</sub> (4.0 mmol), ethanol (12 mL), catalyst (1 mg, 8.23 × 10<sup>-3</sup> mmol% Pd), temperature (80 °C), time (0.5 h).

**Table 2**

Optimization of the catalyst amount in Suzuki-Miyaura coupling reaction promoted by Fe<sub>3</sub>O<sub>4</sub>@La-MOF-Schiff base-Pd.

Entry	Catalyst (mg)	Yield (%)
1	3	95
2	5	98
3	8	>99
4	10	>99
5	15	>99
6	20	>99

Reaction conditions: bromobenzene (1.0 mmol), phenylboronic acid (1.2 mmol), K<sub>2</sub>CO<sub>3</sub> (2.0 mmol), ethanol (6 mL), catalyst Fe<sub>3</sub>O<sub>4</sub>@La-MOF-Schiff-Pd, temperature 80 °C, time 0.5 h.

**Table 3**

Evaluation of main reaction parameters (temperature and time) for the Suzuki-Miyaura coupling reaction with the Fe<sub>3</sub>O<sub>4</sub>@La-MOF-Schiff base-Pd catalyst.

Entry	T (°C)	Time (h)	Yield (%)
1	40	1/2	52
2	60	1/2	89
3	80	1/6	93
4	80	1/3	95
5	80	1/2	>99

Reaction conditions: bromobenzene (1.0 mmol), phenylboronic acid (1.2 mmol), K<sub>2</sub>CO<sub>3</sub> (2.0 mmol), ethanol (6 mL), catalyst (8 mg).

the 88% yield was obtained, corresponding to a high turnover number (TON) of 21,443 and turnover frequency (TOF) of 42,886 h<sup>-1</sup>. Both values are by far superior to other heterogeneous based-MOFs Pd catalysts (e.g. TON of 15,800 and TOF of 1317 for the Mo<sup>II</sup> cluster coordination polymer/Pd<sup>II</sup>Pd<sub>0.6</sub><sup>0</sup>; TOFs of: 396 for Pd/MIL-53 (Al)-NH<sub>2</sub>, 2190.5 for Pd/UiO-66-NH<sub>2</sub>, 2037 for IRMOF-3-PI-Pd, 1235 for UiO-67-3-PI-Pd) [29]. More importantly, our TOF ranks second among highest values communicated for crystalline MOF-Pd catalysts in the Suzuki-Miyaura cross-coupling of bromobenzene and is very close to the best so far reported (43,890, for Pd/AZC) [30].

A heterogeneity test was carried out as well. First, the reaction between bromobenzene and phenylboronic acid was run under above optimal conditions giving >99% yield. The supernatant was then added to the regular mixture of *p*-bromotoluene and phenylboronic and let to react without further addition of catalyst. As expected, no product was detected in this reaction. Consequently, the reaction proceeds solely in heterogeneous mode, with no leaching of Pd ions in the supernatant.

Recyclability of the catalyst was tested in the reaction of iodobenzene and phenylboronic acid, in consecutive runs, separating the catalyst with an external magnet after each run (Fig. 8). It was found that the Fe<sub>3</sub>O<sub>4</sub>@La-MOF-Schiff base-Pd could be reused twelve times without a significant decrease in the yield. The elemental mappings and TEM images of the recovered catalyst show that palladium ions were still evenly distributed in the composite (Figs. 6 and 7). The valence +2 of Pd was maintained (from XPS), indicating that no Pd(0) nanoparticles have been generated during the catalytic process (Fig. S10). According to PXRD tests (Fig. 2) the crystalline phase and catalyst structure were fully preserved in the used catalyst. Therefore, Fe<sub>3</sub>O<sub>4</sub>@La-MOF-Schiff base-Pd proved to be a quite robust, high-performance heterogeneous catalyst for activating aromatic C–X (X = Br, I) bonds in Suzuki-Miyaura cross-coupling reactions.

To account for the superior behaviour of our catalyst we assume that La ions, due to their electropositive propensity, hard Lewis acid character and their key role in building a rigid 3D configuration by multiple coordination modes, enhance the stability of the Pd complex. The latter process occurs *via* a synergistic cooperation of the oxophilic La ions and the aromatic organic linker in transferring charge density to the N–Pd bond (Fig. S7). By this electronic

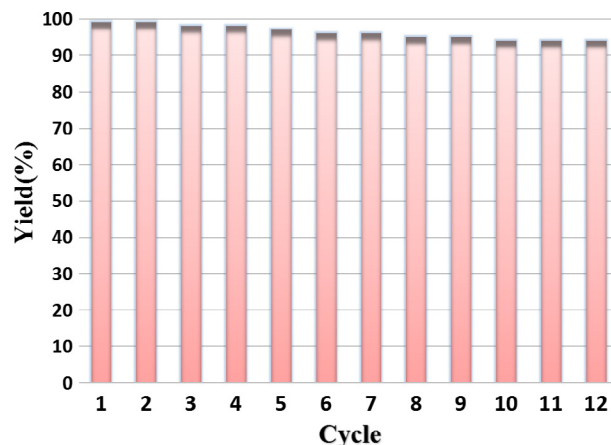
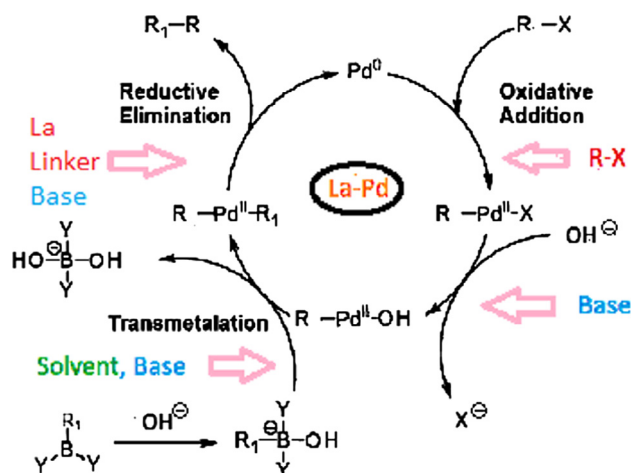


**Fig. 8.** Recycling of Fe<sub>3</sub>O<sub>4</sub>@La-MOF-Schiff base-Pd in Suzuki-Miyaura cross-coupling (under optimal reaction conditions: Table 1, entry 1).



**Scheme 2.** Proposed interaction of La, organic linker, solvent and base within the Pd-catalytic cycle.

effect, La nodes could as well accelerate the reductive elimination step, favouring generation of Pd(0) species able to resume a new catalytic cycle. This kinetic behaviour has been also evidenced in previous reports on La-MOF-Pd catalyzed cross-couplings. [18b,19b] Scheme 2 gives insight into the role of La and organic linker within the Pd catalytic cycle, essentially distinct from that of the substrate, base and solvent [21b–21d].

Along with the kinetic effect, a stronger N–Pd bond that increases the stability of the Pd complex, may substantially diminish Pd leaching in the overall catalytic process. Furthermore, La ions foster a tridimensional MOF architecture with channels and pores favouring decoration with Fe<sub>3</sub>O<sub>4</sub> NP. Post-synthetic modification *via* a Schiff-base to coordinatively bind Pd ions in a uniform and stable arrangement results in an innovative, highly active catalyst.

#### 4. Conclusions

This catalyst demonstrated important beneficial attributes: (a) accessibility from largely available reagents, by a straightforward synthetic protocol which leaves only innocuous residues; (b) robustness of the La-MOF template due to a rigid configuration ensured by the oxophilic lanthanide nodes and the nucleophilic organic linker; (c) superior catalytic activity as evidenced by the quantitative yields and high TONs and TOFs attained at low

catalyst loadings, under mild reaction conditions; (d) easy recoverability using external permanent magnets; and, quite importantly: (e) proven recyclability for at least 12 runs without significant loss of the catalytic activity. These merits recommending the Fe<sub>3</sub>O<sub>4</sub>@La-MOF-Schiff base-Pd promoter for user-friendly, economical C–C cross-couplings are poised to contribute to the development of high-performance heterogeneous palladium catalytic systems.

## Acknowledgements

This work was supported by the Natural Science Foundation of China (21671139 and 21501122), the Distinguished Professor Project of Liaoning Province (2013204) and Doctoral Scientific Research Foundation of Liaoning Province (201601193). Natural Science Foundation of Liaoning Province (20170540713) and Liaoning Province Department of Education Fund (LFD2017001). F.D. acknowledges the Chinese Scholarship Council ([2012]5031) for financial support. I.D. and V.D. gratefully acknowledge support from the Romanian Academy, Institute of Organic Chemistry, Bucharest, Romania.

## Appendix A. Supplementary data

Supplementary data associated with this article can be found, in the online version, at <https://doi.org/10.1016/j.jcat.2018.02.026>.

## References

- (a) Y.-B. Huang, J. Liang, X.-S. Wang, R. Cao, Multifunctional metal-organic framework catalysts: synergistic catalysis and tandem reactions, *Chem. Soc. Rev.* 46 (2017) 126; (b) J. Chen, K. Shen, Y. Li, Greening the processes in MOFs synthesis and MOFs-involved sustainable catalysis, *ChemSusChem* 10 (2017) 3165; (c) L. Oar-Arteta, T. Wezendonk, X. Sun, F. Kapteijn, J. Gascon, Metal organic frameworks as precursors for the manufacture of advanced catalytic materials, *Mater. Chem. Front.* 1 (2017) 1709; (d) A. Dhakshinamoorthy, A.M. Asiri, H. Garcia, Mixed-metal or mixed-linker metal organic frameworks as heterogeneous catalysts, *Catal. Sci. Technol.* 6 (2016) 5238; (e) W.H. Dong, L. Zhang, C.H. Wang, C. Feng, N.Z. Shang, S.T. Gao, C. Wang, Palladium nanoparticles embedded in metal-organic framework derived porous carbon: synthesis and application for efficient Suzuki-Miyaura coupling reactions, *RSC Adv.* 6 (2016) 37118; (f) Y.-B. Huang, M. Shen, X. Wang, P. Huang, R. Chen, Z.-J. Lin, R. Cao, Water-medium C-H activation over a hydrophobic perfluoroalkane-decorated metal-organic framework platform, *J. Catal.* 333 (2016) 1; (g) Y. Zhang, J.Y. Ying, Main-chain organic frameworks with advanced catalytic functionalities, *ACS Catal.* 5 (2015) 2681.
- (a) I. Schwedler, S. Henke, M.T. Wharmby, S.R. Bajpe, A.K. Cheetham, R.A. Fischer, Mixed-linker solid solutions of functionalized pillared-layer MOFs—adjusting structural flexibility, gas sorption, and thermal responsiveness, *Dalton Trans.* 45 (2016) 4230; (b) G. Chang, B. Li, H. Wang, T. Hu, Z. Bao, B. Chen, Control of interpenetration in a microporous metal-organic framework for significantly enhanced C<sub>2</sub>H<sub>2</sub>/CO<sub>2</sub> separation at room temperature, *Chem. Commun.* 52 (2016) 3494; (c) T.R.C. Van Assche, G.V. Baron, J.F.M. Denayer, Molecular separations with breathing metal-organic frameworks: modelling packed bed adsorbers, *Dalton Trans.* 45 (2016) 4416; (d) Z. Chen, K. Adil, Ł.J. Weseliński, Y. Belmabkhout, M. Eddaoudi, A supermolecular building layer approach for gas separation and storage applications: the eea and rtl MOF platforms for CO<sub>2</sub> capture and hydrocarbon separation, *J. Mater. Chem. A* 3 (2015) 6276; (e) Y. He, W. Zhou, G. Qian, B. Chen, *Chem. Soc. Rev.* 43 (2014) 5657; (f) E. Barea, C. Montoro, J.A.R. Navarro, Toxic gas removal-metal-organic frameworks for the capture and degradation of toxic gases and vapours, *Chem. Soc. Rev.* 43 (2014) 5419.
- (a) F. Ke, Y.P. Yuan, L.G. Qiu, Y.H. Shen, A.J. Xie, J.F. Zhu, X.Y. Tian, L.D. Zhang, Facile fabrication of magnetic metal-organic framework nanocomposites for potential targeted drug delivery, *J. Mater. Chem.* 21 (2011) 3843; (b) J.W. Cao, Y.F. Gao, Y.Q. Wang, C.F. Du, Z.L. Liu, A microporous metal-organic open framework containing uncoordinated carbonyl groups as postsynthetic modification sites for cation exchange and Tb<sup>3+</sup> sensing, *Chem. Commun.* 49 (2013) 6897.
- (a) D. Zhao, Y. Cui, Y. Yang, G. Qian, *CrystEngComm* 18 (2016) 3746; (b) Y.-N. Wang, P. Zhang, J.-H. Yu, J.-Q. Xu, 4-(4-Carboxyphenoxy) phthalate-based coordination polymers and their application in sensing nitrobenzene, *Dalton Trans.* 44 (2015) 1655; (c) Z. Hu, B. Deibert, J. Li, Luminescent metal-organic frameworks for chemical sensing and explosive detection, *Chem. Soc. Rev.* 43 (2014) 5815; (d) J. Liu, L. Chen, H. Cui, J. Zhang, L. Zhang, C.-Y. Su, Applications of metal-organic frameworks in heterogeneous supramolecular catalysis, *Chem. Soc. Rev.* 43 (2014) 6011; (e) P. Ramaswamy, N.E. Wong, G.K.H. Shimizu, MOFs as proton conductors—challenges and opportunities, *Chem. Soc. Rev.* 43 (2014) 5913; (f) V. Stavila, A.A. Talin, M.D. Allendorf, MOF-based electronic and optoelectronic devices, *Chem. Soc. Rev.* 43 (2014) 5994.
- (a) A. Dhakshinamoorthy, A.M. Asiri, H. Garcia, Metal-organic frameworks as heterogeneous catalysts in liquid phase reactions: why are they so exceptional?, *Chimica Oggi* 33 (2015) 40; (b) K Meyer, M. Ranocchiari, J.A. van Bokhoven, Metal organic frameworks for photo-catalytic water splitting, *Energy Environ. Sci.* 8 (2015) 1923; (c) A. Dhakshinamoorthy, H. Garcia, Metal-organic frameworks as solid catalysts for the synthesis of nitrogen-containing heterocycles, *Chem. Soc. Rev.* 43 (2014) 5750; (d) T. Zhang, W. Lin, Metal-organic frameworks for artificial photosynthesis and photocatalysis, *Chem Soc. Rev.* 43 (2014) 5982.
- C. Chen, C.A. Allen, S.M. Cohen, Tandem postsynthetic modification of metal-organic frameworks using an inverse-electron-demand Diels-Alder reaction, *Inorg. Chem.* 50 (2011) 10534.
- J. Canivet, S. Aguado, Y. Schuurman, D. Farrusseng, MOF-supported selective ethylene dimerization single-site catalysts through one-pot postsynthetic modification, *J. Am. Chem. Soc.* 135 (2013) 4195.
- B. Li, Y.M. Zhang, D.X. Ma, L. Li, G.G. Li, G.D. Li, Z. Shi, S.H. Feng, A strategy toward constructing a bifunctionalized MOF catalyst: post-synthetic modification of MOFs on organic ligands and coordinatively unsaturated metal sites, *Chem. Commun.* 48 (2012) 6151.
- S.M. Cohen, Postsynthetic methods for the functionalization of metal-organic frameworks, *Chem. Rev.* 112 (2012) 970.
- K.K. Tanabe, S.M. Cohen, Postsynthetic modification of metal-organic frameworks—a progress report, *Chem. Soc. Rev.* 40 (2011) 498.
- S.J. Garibay, S.M. Cohen, Isoreticular synthesis and modification of frameworks with the UiO-66 topology, *Chem. Commun.* 46 (2010) 7700.
- K. Peikert, F. Hoffmann, M. I Froba, Amino substituted Cu<sub>3</sub>(btc)<sub>2</sub>: a new metal-organic framework with a versatile functionality, *Chem. Commun.* 48 (2012) 11196.
- J.W. Brown, N.N. Jarenwattananon, T. Otto, J.L. Wang, S. Glöggler, L.S. Bouchard, Heterogeneous Heck coupling in multivariate metal-organic frameworks for enhanced selectivity, *Catal. Commun.* 65 (2015) 105.
- Z.G. Sun, G. Li, H.O. Liu, L.P. Liu, Salen-Co(II) complex incorporated into amino-functionalized MIL-101(Cr) through postsynthetic modification as a cooperative catalyst for cyclohexane selective oxidation, *Appl. Catal. A: Gen.* 466 (2013) 98.
- C.J. Doonan, W. Morris, H. Furukawa, O.M. Yaghi, Isoreticular metalation of metal-organic frameworks, *J. Am. Chem. Soc.* 131 (2009) 9492.
- (a) C. Rösler, R.A. Fischer, Metal-organic frameworks as hosts for nanoparticles, *CrystEngComm* 17 (2015) 199; (b) J. Zhao, X. He, Y. Zhang, J. Zhu, X. Shen, D. Zhu, Highly water stable lanthanide metal-organic frameworks constructed from 2,2′-Disulfonyl-4,4′-biphenyldicarboxylic Acid: Syntheses, Structures, and Properties, *Cryst. Growth Des.* 17 (2017) 5524.
- (a) J.G. de Vries, Palladium-Catalyzed Coupling Reactions, in: M. Beller, H.-U. Blaser (Eds.), *Organometallics as Catalysts in the Fine Chemical Industry*, Springer-Verlag, Berlin, Heidelberg, Germany, 2012, pp. 1–34; (b) C. Torborg, M. Beller, Recent applications of palladium-catalyzed coupling reactions in the pharmaceutical, agrochemical, and fine chemical industries, *Adv. Synth. Catal.* 351 (2009) 3027; (c) A. Chatterjee, T.R. Ward, Recent advances in the palladium catalyzed Suzuki-Miyaura cross-coupling reaction in water, *Catal. Lett.* 146 (2016) 820.
- (a) P. Gautam, B.M. Bhanage, *J. Org. Chem.* 80 (2015) 7810; (b) L. You, W. Zhu, S. Wang, G. Xiong, F. Ding, B. Ren, I. Dragutan, V. Dragutan, Y.G. Sun, High catalytic activity in aqueous Heck and Suzuki-Miyaura reactions catalyzed by novel Pd/Ln coordination polymers based on 2,2′-bipyridine-4,4′-dicarboxylic acid as a heteroleptic ligand, *Polyhedron* 115 (2016) 47; (c) R.D.J. Froese, Ch. Lombardi, M. Pompeo, R.P. Rucker, M.G. Organ, Designing Pd–N-heterocyclic carbene complexes for high reactivity and selectivity for cross-coupling applications, *Acc. Chem. Res.* 50 (2017) 2244.
- (a) S.L. Huang, A.Q. Jia, G.X. Jin, Pd(diimine)Cl<sub>2</sub> embedded heterometallic compounds with porous structures as efficient heterogeneous catalysts, *Chem. Commun.* 49 (2013) 2403; (b) L. You, W. Zong, G. Xiong, F. Ding, S. Wang, B. Ren, I. Dragutan, V. Dragutan, Y.-G. Sun, Cooperative effects of lanthanides when associated with palladium in novel, 3D Pd/Ln coordination polymers. Sustainable applications as water-stable, heterogeneous catalysts in carbon-carbon cross-coupling reactions, *Appl. Catal. A Gen.* 511 (2016) 1; (c) L.-X. You, H.-J. Liu, L.-X. Cui, F. Ding, G. Xiong, S.-J. Wang, B.-Y. Ren, I. Dragutan, V. Dragutan, Y.-G. Sun, The synergistic effect of cobalt on a Pd/Co catalyzed Suzuki-Miyaura cross-coupling in water, *Dalton Trans.* 45 (2016) 18455.
- (a) V. Ramakrishna, N. Dastagiri Reddy, Synthesis of zwitterionic palladium complexes and their application as catalysts in cross-coupling reactions of aryl, heteroaryl and benzyl bromides with organoboron reagents in neat water, *Dalton Trans.* 46 (2017) 8598;

- (b) L.F. Liu, Y.H. Zhang, Y.G. Wang, Phosphine-free palladium acetate catalyzed Suzuki reaction in water, *J. Org. Chem.* 70 (2005) 6122.
- [21] (a) Á. Molnár, A. Papp, Catalyst recycling—a survey of recent progress and current status, *Coord. Chem. Rev.* 349 (2017) 1;  
(b) Q.B. Liang, P. Xing, Z.G. Huang, J.J. Dong, K.B. Sharpless, X.X. Li, B. Jiang, Palladium-catalyzed, ligand-free Suzuki reaction in water using aryl fluorosulfates, *Org. Lett.* 17 (2015) 1942;  
(c) C.F.R.A.C. Lima, A.S.M.C. Rodrigues, V.L.M. Silva, A.M.S. Silva, L.M.N.B.F. Santos, Role of the base and control of selectivity in the Suzuki-Miyaura cross-coupling reaction, *ChemCatChem* 6 (2014) 1291;  
(d) Ch. Amatore, G. Le Duc, A. Jutand, Mechanism of palladium-catalyzed Suzuki-miyaura reactions: multiple and antagonistic roles of anionic “Bases” and their counterions, *Chem. Eur. J.* 19 (2013) 10082;  
(e) Ch. Amatore, A. Jutand, G. Le Duc, Mechanistic origin of antagonist effects of usual anionic bases ( $\text{OH}^-$ ,  $\text{CO}_3^{2-}$ ) as modulated by their counterions ( $\text{Na}^+$ ,  $\text{Cs}^+$ ,  $\text{K}^+$ ) in palladium-catalyzed Suzuki-Miyaura reactions, *Chem. Eur. J.* 18 (2012) 6616.
- [22] S. Sobhani, Z.M. Falatoni, S. Asadi, M. Honarmand, Palladium-schiff base complex immobilized covalently on magnetic nanoparticles as an efficient and recyclable catalyst for Heck and Suzuki cross-coupling reactions, *Catal. Lett.* 146 (2016) 255.
- [23] (a) Y.Q. Zhang, X.W. Wei, R. Yu,  $\text{Fe}_3\text{O}_4$  nanoparticles-supported palladium-bipyridine complex: effective catalyst for Suzuki coupling reaction, *Catal. Lett.* 135 (2010) 256;  
(b) D. Wang, C. Deraedt, L. Salmon, C. Labrugere, L. Etienne, J. Ruiz, D. Astruc, Efficient and magnetically recoverable “Click” PEGylated  $\gamma\text{-Fe}_2\text{O}_3$ -Pd nanoparticle catalysts for Suzuki-Miyaura, Sonogashira, and Heck reactions with positive dendritic effects, *Chem. Eur. J.* 21 (2015) 1508;  
(c) D. Yuan, H. Zhang, Nanosized palladium supported on diethylenetriamine modified superparamagnetic polymer composite microspheres: synthesis, characterization and application as catalysts for the Suzuki reactions, *Appl. Catal. A Gen.* 475 (2014) 249;
- (d) M.O. Sydnes, Use of nanoparticles as catalysts in organic synthesis—cross-coupling reactions, *Curr. Org. Chem.* 18 (2014) 312;  
(e) M.O. Sydnes, The Use of Palladium on magnetic support as catalyst for Suzuki-Miyaura cross-coupling reactions, *Catalysts* 7 (2017) 35.
- [24] Y. Luo, G. Calvez, S. Freslon, C. Daiguebonne, T. Roisnel, O. Guillou, A family of lanthanide-containing molecular open frameworks with high porosity:  $[\text{Ln}(\text{abdc})(\text{H}_2\text{O})_n]_\infty$  with  $\text{Ln} = \text{La-Eu}$  and  $8 \leq n \leq 11$ , *Inorg. Chim. Acta* 368 (2011) 170.
- [25] J.H. Yang, D.F. Wang, W.D. Liu, X. Zhang, F.L. Bian, W. Yu, Palladium supported on a magnetic microgel: an efficient and recyclable catalyst for Suzuki and Heck reactions in water, *Green Chem.* 15 (2013) 3429.
- [26] J.P. Huang, W. Wang, H.X. Li, Water-medium organic reactions catalyzed by active and reusable Pd/Y heterobimetal-organic framework, *ACS Catal.* 3 (2013) 1526.
- [27] X.Y. Chen, B. Zhao, W. Shi, J. Xia, P. Cheng, D.Z. Liao, S.P. Yan, Z.H. Jiang, Microporous metal-organic frameworks built on a  $\text{Ln}_3$  cluster as a six-connecting node, *Chem. Mater.* 17 (2005) 2866.
- [28] T. Ichikawa, M. Netsu, M. Mizuno, T. Mizusaki, Y. Takagi, Y. Sawama, Y. Monguchi, H. Sajiki, Development of a unique heterogeneous palladium catalyst for Suzuki-Miyaura reaction using (hetero) aryl chlorides and chemoselective hydrogenation, *Adv. Synth. Catal.* 13 (2017) 2269.
- [29] R. Sun, B. Liu, B.G. Li, S. Jie, Palladium(II)@zirconium-based mixed-linker metal-organic frameworks as highly efficient and recyclable catalysts for Suzuki and Heck cross-coupling reactions, *ChemCatChem* 8 (2016) 3261.
- [30] H. Choudhary, S. Nishimura, K. Ebitani, Tailored design of palladium species grafted on an amino functionalized organozinc coordination polymer as a highly pertinent heterogeneous catalyst, *J. Mater. Chem. A* 2 (2014) 18687.